Inorg. Chem. **1994**, *33*, 428–433

Modeling the Photosynthetic Water Oxidation Center: Synthesis, Structure, and Magnetic Properties of $[Mn_2(\mu\text{-}O)_2(\mu\text{-}OAc)(H_2O)_2(bipy)_2](ClO_4)_3\cdot H_2O$

K. R. Reddy,[†] M. V. Rajasekharan,[*,†] S. Padhye,[*,‡] F. Dahan,[§] and J.-P. Tuchagues[*,§]

School of Chemistry, University of Hyderabad, Hyderabad 500134, India, Department of Chemistry,
University of Poona, Pune 411007, India, and Laboratoire de Chimie de Coordination du CNRS,
UP 8241 liée par conventions à l'Université Paul Sabatier et à l'Institut National Polytechnique,
205 route de Narbonne, 31077 Toulouse Cedex, France

Received June 18, 1993[◉]

$[Mn_2(\mu\text{-}O)_2(\mu\text{-}OAc)(H_2O)_2(bipy)_2](ClO_4)_3\cdot H_2O$ crystallizes in the monoclinic system, space group $P2_1/n$ (No. 14) with $Z = 4$ and $a = 13.619(1)$ Å, $b = 16.213(2)$ Å, $c = 16.266(1)$ Å, and $\beta = 113.08(1)°$. The structure was solved by direct methods and refined to conventional agreement indices $R = 0.021$ and $R_w = 0.024$ with 5159 unique reflections for which $I > 3\sigma(I)$. The structure consists of binuclear $[Mn^{IV}_2(\mu\text{-}O)_2(\mu\text{-}OAc)(H_2O)_2(bipy)_2]^{3+}$ cations separated by ClO_4^- anions and a molecule of water of crystallization. This dimanganese(IV) compound is the first to include simultaneously a bridging acetato ligand, a bis(μ-oxo) bridge and two water molecules, each directly coordinated to one manganese(IV) ion. This high-valent bis(μ-oxo)–μ-acetato-bridged binuclear species has been studied with optical and EPR spectroscopy. The analysis of the thermal variation of its magnetic susceptibility affords one of the weakest antiferromagnetic interaction ($J = -43.7$ cm^{-1}, $\mathcal{H} = -2JS_1S_2$) determined for a bis(μ-oxo)-bridged Mn^{IV}_2 species. The weakening of the antiferromagnetic interaction is tentatively correlated to the departure of the $Mn^{IV}(\mu\text{-}O)_2Mn^{IV}$ ring from planarity (18.3°) as a result of the constraint exerted by the μ-acetato bridge.

Introduction

The identification of a polynuclear manganese-containing site in photosystem II (PSII) has stimulated considerable research in the coordination compounds of high-valent manganese.[1] The manganese cluster in PSII of plants is known to cycle between five distinct oxidation levels labeled as S_n states[2,3] which contain manganese ions in various combinations of oxidation states, including Mn^{II}, Mn^{III}, and Mn^{IV} while ligation is provided by O and N atoms from amino acid residues.[4] A variety of ligating systems has been employed to attain the high-valent manganese states and mimick the structural features of the active site. Of these, the manganese-bipyridine system has provided several well-characterized compounds.

Following the first preparation of $[(bipy)_2Mn(O)_2Mn(bipy)_2](S_2O_8)_{1.5}$ by Nyholm and Turco,[5] the mixed-valence dimer $[(bpy)_2Mn(\mu\text{-}O)_2Mn(bpy)_2]^{3+}$ has been studied extensively as a model for the oxygen-evolving complex of PSII.[6]

Introduction of the carboxylate group as a manganese-bridging moiety in the above dimeric species has tremendously expanded the scope and type of compounds that can be prepared from this system.[7] Some of the recently reported compounds belonging to the manganese–acetate–bipyridine system include $[Mn^{III}Mn^{IV}(O)_2(OAc)Cl_2(bipy)_2]$,[8] $[Mn^{III}_4(O)_2(OAc)_7(bipy)_2]^+$,[9] $[Mn^{III}_2O(OAc)_2(bipy)_2(H_2O)_2]^{2+}$,[10] $[Mn^{III}_2O(OAc)_2(bipy)_2Cl_2]$,[7] $[Mn^{III}_2O(OAc)_2(bipy)_2(H_2O)(S_2O_8)]$,[11] $[Mn^{II}_2Mn^{III}_2(OAc)_6(bipy)_2]$,[9] $[Mn^{II}_3(OAc)_6(bipy)_2]$,[12] and $[LMn^{IV}(O)_2(OAc)Mn^{III}(bipy)(MeOH)]^{2+}$ (L = 1,4,7-trimethyl-1,4,7-triazacyclononane).[13] It has been shown that the mixed-valence complex $[Mn_2(O)_2(bipy)_4]^{3+}$ disproportionates in strongly acidic solution, leading to isolation of a trinuclear complex, $[Mn^{IV}_3(O)_4(bipy)_4(H_2O)_2]^{4+}$.[14] Similarly, Sarneski *et al.*[15] have obtained a phosphate-bridged

---

[*] To whom correspondence should be addressed.

[†] University of Hyderabad.

[‡] University of Poona.

[§] Laboratoire de Chimie de Coordination du CNRS.

[◉] Abstract published in *Advance ACS Abstracts,* December 15, 1993.

(1) For recent reviews, see: Mulay, M.; Padhye, S. *Proc. Indian Natl. Sci. Acad.* **1987**, *B53*, 471. Pecoraro, V. L. *Photochem. Photobiol.* **1988**, *48*, 249–264. Rutherford, A. W. *Trends Biochem. Sci.* **1989**, *14*, 227–232. Vincent, J. B.; Christou, G. *Adv. Inorg. Chem.* **1989**, *33*, 197–257. Wieghardt, K. *Angew. Chem., Int. Ed. Engl.* **1989**, *28*, 1153–1172. Brudvig, G. W.; Crabtree, R. H. *Prog. Inorg. Chem.* **1989**, *37*, 99–142. Dismukes, G. C. *Photochem. Photobiol.* **1986**, *43*, 99–115. Brudvig, G. W. In *Metal Clusters in Proteins*; Que, L., Jr., Ed.; ACS Symposium Series 372; American Chemical Society: Washington, DC, 1988; pp 221–237.

(2) Joliot, P.; Barbieri, G.; Chabaud, R. *Photochem. Photobiol.* **1969**, *10*, 302.

(3) Kok, B.; Forbush, B.; Mc Gloin, M. P. *Photochem. Photobiol.* **1970**, *11*, 457–475.

(4) (a) Amesz, J. *Biochim. Biophys.* **1983**, *726*, 1–12. (b) Takohashi, Y.; Katoh, S. *Biochim. Biophys. Acta* **1986**, *848*, 183. (c) Yachandra, V. K.; Guiles, R. D.; Mc Dermott, A.; Britt, R. D.; Dexheimer, S. L.; Sauer, K.; Klein, M. P. *Biochim. Biophys. Acta* **1986**, *850*, 324. (d) Guiles, R. D.; Yachandra, V. K.; Mc Dermott, A. E.; Britt, R. D.; Dexheimer, S. L.; Sauer, K.; Klein, M. P. In *Proceedings of the VII International Congress on Photosynthesis*; Biggens, J., ed., Progress in Photosynthesis Research 1; Martinus Nijhoff Publishers: Dordrecht, The Netherlands, 1987. (e) Tamura, N.; Ikeuchi, M.; Inoue, Y. *Biochim. Biophys. Acta* **1989**, *973*, 281–289. (f) Guiles, R. D.; Zimmerman, J. L.; McDermott, A. E.; Yachandra, V. K.; Cole, J. L.; Dexheimer, S. L.; Britt, R. D.; Wieghardt, K.; Bossek, U.; Sauer, K.; Klein, M. P. *Biochemistry* **1990**, *29*, 471–485. (g) De Rose, V. J.; Yachandra, V. K.; Mc Dermott, A. E.; Britt, R. D.; Sauer, K.; Klein, M. D. *Biochemistry* **1991**, *30*, 1335–1341.

(5) Nyholm, R. S.; Turco, A. *Chem. Ind.* **1960**, 74.

(6) (a) Cooper, S. R.; Dismukes, G. C.; Klein, M. P.; Calvin, M. *J. Am. Chem. Soc.* **1978**, *100*, 7248. (b) Inoue, M. *Bull. Chem. Soc. Jpn.* **1978**, *51*, 1400. (c) Cooper, S. R.; Calvin, M. *J. Am. Chem. Soc.* **1977**, *99*, 6623. (d) Plaskin, P. M.; Stoufer, R. C.; Mathew, M.; Palenik, G. J. *J. Am. Chem. Soc.* **1972**, *94*, 1121–1122. (e) Stebler, M.; Ludi, A.; Bürgi, H. B. *Inorg. Chem.* **1986**, *25*, 4743–4750. (f) Morrison, M. M.; Sawyer, D. T. *J. Am. Chem. Soc.* **1977**, *99*, 257–258.

(7) Christou, G. *Acc. Chem. Res.* **1989**, *22*, 328–335.

(8) Bashkin, J. S.; Schake, A. R.; Vincent, J. B.; Chang, H. R.; Li, Q.; Huffman, J. C.; Christou, G.; Hendrickson, D. N. *J. Chem. Soc., Chem. Commun.* **1988**, 700–702.

(9) Vincent, J. B.; Christmas, C.; Chang, H. R.; Li, Q.; Boyd, P. D. W.; Huffman, J. C.; Hendrickson, D. N.; Christou, G. *J. Am. Chem. Soc.* **1989**, *111*, 2086–2097.

(10) Menage, S.; Girerd, J. J.; Gleizes, A. *J. Chem. Soc., Chem. Commun.* **1988**, 431–432.

(11) Blackman, A. G.; Huffman, J. C.; Lobkovsky, E. B.; Christou, G. *J. Chem. Soc., Chem. Commun.* **1991**, 989–991.

(12) Menage, S.; Vitols, S. E.; Bergerat, P.; Codjovi, E.; Kahn, O.; Girerd, J. J.; Guillot, M.; Solans, X.; Calvet, T. *Inorg. Chem.* **1991**, *30*, 2666–2671.

(13) Bossek, U.; Saher, M.; Weyhermüller, T.; Wieghardt, K. *J. Chem. Soc., Chem. Commun.* **1992**, 1780–1782.

(14) Sarneski, J. E.; Thorp, H. H.; Brudvig, G. W.; Crabtree, R. H.; Schuttle, G. K. *J. Am. Chem. Soc.* **1990**, *112*, 7255–7260.

0020-1669/94/1333-0428$04.50/0

Mn^{IV}_2 complex, $[Mn^{IV}_2(O)_2(\mu\text{-}HPO_4)(bipy)_2(H_2PO_4)_2]$ by treating an aqueous solution of the mixed-valence dimer with H_3PO_4.

We present here the synthesis, crystal structure and magnetic properties of the acetato-bridged Mn^{IV}_2 complex ion, $[Mn^{IV}_2(\mu\text{-}O)_2(\mu\text{-}OAc)(H_2O)_2(bipy)_2]^{3+}$ following a procedure involving oxidation of Mn^{2+} by Ce^{4+} in the presence of acetate and bipyridine ligands.

Experimental Section

Preparation of $[Mn_2(\mu\text{-}O)_2(\mu\text{-}OAc)(H_2O)_2(bipy)_2](ClO_4)_3\cdot H_2O$. 2,2′-Bipyridine (600 mg) was added to a solution of $Mn(CH_3COO)_2\cdot 4H_2O$ (500 mg) in 20 mL of water and 3 mL of acetic acid. After dissolution of the ligand, a solution of ceric perchlorate (10 mL) (obtained by dissolving freshly precipitated ceric hydroxide in a minimum amount of concentrated perchloric acid) was added. The resulting light brown solution was filtered and set aside for a week to obtain 280 mg of well-formed crystals of the dimer. Anal. Calcd for $Mn_2C_{22}H_{25}N_4O_{19}Cl_3$: C, 30.52; H, 2.91; N, 6.47. Found: C, 29.96; H, 3.07; N, 6.15. Equivalent weight (by iodometry): 217, in good agreement with the calculated value of 216.

Physical Measurements. Element analyses were carried out at the microanalytical laboratory of the University of Hyderabad for C, H, and N.

Electronic spectra were measured using a Shimadzu Model 200S UV-vis spectrophotometer, and EPR measurements were performed on a JEOL FE3X spectrometer.

Variable-temperature magnetic susceptibility data were obtained on powdered polycrystalline samples with a Quantum Design MPMS SQUID susceptometer. Diamagnetic corrections were applied by using Pascal's constants. Least-squares computer fittings of the magnetic susceptibility data were accomplished with an adapted version of the function-minimization program STEPT.[16]

X-ray Crystal Structure Determination. A dark brown nearly cubic crystal (0.50 × 0.45 × 0.40 mm) was sealed on a glass fiber and mounted on an Enraf-Nonius CAD 4 diffractometer. A total of 7480 reflections (7189 unique) in two octants $(hkl,hk\bar{l})$ with $2\theta \le 54°$ were collected at 22 °C using Mo Kα radiation with a graphite monochromator (λ = 0.710 73 Å). The crystal of $[Mn_2(\mu\text{-}O)_2(\mu\text{-}OAc)(H_2O)_2(bipy)_2](ClO_4)_3\cdot H_2O$ belongs to the monoclinic system and its space group was assigned as $P2_1/n$ from extinctions $h0l, h + 1 = 2n + 1$, and $0k0, k = 2n + 1$. The crystal quality was monitored by scanning three standard reflections every 2 h. No significant variation was observed during the data collection. After corrections for Lorentz and polarization effects,[17] an empirical absorption correction was applied.[18] A total of 7189 independent reflections were obtained on averaging in $P2_1/n$. Cell constants were obtained from a least-squares fit of 25 reflections.

Structure Solution and Refinement. The structure was solved by using direct methods.[19] With a final data set of 5159 reflections ($I > 3\sigma(I)$), non-hydrogen atoms were located in successive Fourier difference maps and least-squares refinement cycles.[20] Three oxygen atoms of a perchlorate anion are disordered. Their site occupancy factors were refined, and the model finally kept included two orientations with a 50% occupancy ratio. All non-hydrogen atoms were refined anisotropically. Hydrogen atoms were found in a difference Fourier synthesis. The hydrogen atoms of the water molecules were refined while the other were included in calculations with a constrained geometry (C–H = 0.97 Å). Hydrogen isotropic temperature factors were first allowed to vary and then kept fixed (0.065 Å^2). The atomic scattering factors and anomalous dispersion terms were taken from the standard compilation.[21] The final full-matrix least-squares refinement converged to $R = 0.021$ and $R_w = 0.024$ with a weighting scheme $w = 1$. The goodness of fit was $s = 1.03$ with 5159 observations and 496 variables.

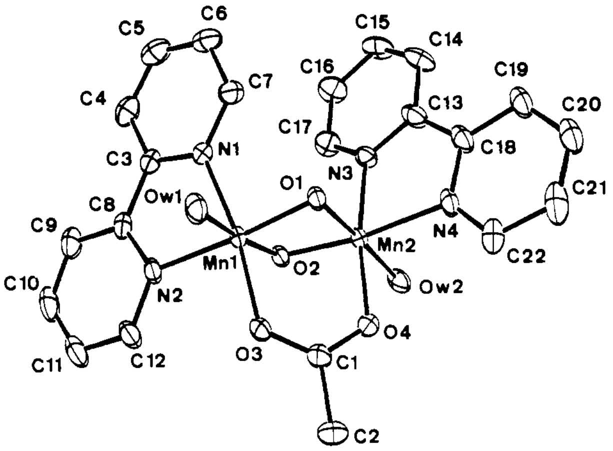

Figure 1. ORTEP view of the $[Mn_2(\mu\text{-}O)_2(\mu\text{-}OAc)(H_2O)_2(bipy)_2]^{3+}$ complex cation.

Table 1. Crystallographic Data for $[Mn_2(\mu\text{-}O)_2(\mu\text{-}OAc)(H_2O)_2(bipy)_2](ClO_4)_3\cdot H_2O$

chemical formula: $Mn_2C_{22}H_{25}N_4O_{19}Cl_3$	fw = 865.69
$a = 13.619(1)$ Å	space group: $P2_1/n$ (No. 14)
$b = 16.213(2)$ Å	$T = 22$ °C
$c = 16.266(1)$ Å	$\lambda = 0.710\ 73$ Å
$\beta = 113.08(1)°$	$\rho_{calc} = 1.74$ g cm^{-3}
$V = 3304.1$ Å^3	μ(Mo Kα) = 10.6 cm^{-1}
$Z = 4$	transm coeff = 0.964–0.999
$R(\sum\|\|F_o\| - \|F_c\|\|)/(\sum\|F_o\|) = 0.021$	$R_w\ ([\sum(\|F_o\| - \|F_c\|)^2/(\sum\|F_o\|)^2]^{1/2}) = 0.024$

All calculations were performed on a MicroVAX 3400 computer using the programs MOLEN,[17] SHELX 76,[20] SHELXS 86[19] and ORTEP.[22] The complex cation of the $[Mn_2(\mu\text{-}O)_2(\mu\text{-}OAc)(H_2O)_2(bipy)_2](ClO_4)_3\cdot H_2O$ molecule is shown in Figure 1 with atom numbering. The crystallographic data are summarized in Table 1. Final fractional atomic coordinates with their estimated standard deviations, selected bond lengths and bond angles are given in Tables 2–4, respectively.

Results and Discussion

Synthesis. Even though it is well-known that oxidation of organic substrates by Ce^{4+} is often catalyzed by Mn^{2+} salts,[23] the synthetic potential of ceric oxidation for the preparation of high-valent manganese complexes has not been fully recognized until now. Our investigations in this direction were prompted by the observation of formation of MnO_4^- species during oxygen evolution experiments using $Mn^{III}Mn^{IV}$–bipyridyl complexes and $(NH_4)_2Ce(NO_3)_6$.[24] Several new high-valent Mn complexes have been isolated using ceric oxidation, the structural characterizations of which are in progress.[25]

Molecular Structure of $[Mn_2(\mu\text{-}O)_2(\mu\text{-}OAc)(H_2O)_2(bipy)_2](ClO_4)_3\cdot H_2O$. The complex molecule defining the asymmetric unit is comprised of one binuclear complex cation, three perchlorate anions, and one water molecule. The central unit of the complex cation consists of two manganese(IV) centers bridged by two μ-oxo and one μ-acetato anions (Figure 1). Due to the presence of the acetato bridge, the four-membered $Mn^{IV}(\mu\text{-}O)_2Mn^{IV}$ ring is not planar (dihedral angle between O(1)Mn(1)O(2) and O(1)Mn(2)O(2) planes = 161.7(1)°). This value is very close to that reported by Armstrong et al.[26] for $[Mn^{IV}_2(\mu\text{-}O)_2(\mu\text{-}OAc)(tpen)](ClO_4)_3$ (tpen = *N,N,N′,N′*-tetrakis(2-pyridyl-

---

(15) Sarneski, J. E.; Didiuk, M.; Thorp, H. H.; Crabtree, R. H.; Brudvig, G. W.; Faller, J. W.; Schuttle, G. K. *Inorg. Chem.* **1991**, *30*, 2833–2835.

(16) Chandler, J. P. Program 66, Quantum Chemistry Program Exchange, Indiana University.

(17) Fair, C. K. *MOLEN, Molecular Structure Solution Procedures*; Enraf-Nonius: Delft, The Netherlands, 1990.

(18) North, A. C. T.; Phillips, D. C.; Mathews, F. S. *Acta. Crystallogr., Sect. A: Found. Crystallogr.* **1968**, *A24*, 351–359.

(19) Sheldrick, G. M. *SHELXS 86. Program for Crystal Structure Solution*; University of Göttingen: Göttingen, Germany, 1986.

(20) Sheldrick, G. M. *SHELX 76. Program for Crystal Structure Determination*; University of Cambridge: Cambridge, England, 1976.

(21) *International Tables for X-ray Crystallography*; Kynoch Press: Birmingham, England, 1974; Vol. IV.

(22) Johnson, C. K. *ORTEP, Report ORNL-3794*, Oak Ridge National Laboratory, Oak Ridge, TN, 1965.

(23) Sharma, Y. R.; Prakash, P. K. S. *Indian J. Chem.* **1980**, *19A*, 1175–1178.

(24) Swarnabala, G.; Rajasekaharan, M. V. *Proc. Natl. Ind. Acad. Sci. (Chem. Sci.)* **1990**, *102*, 87–98.

(25) This includes the previously reported[12] trimer $[Mn_3O_4(bpy)_4(OH_2)_2](ClO_4)_4\cdot 5H_2O$: Reddy, R. K.; Rajasekharan, M. V. *Polyhedron* **1993**, in press.

(26) Pal, S.; Armstrong, W. H. *Inorg. Chem.* **1992**, *31*, 5417–5423.

Table 2. Fractional Atomic Coordinates and Isotropic Equivalent Temperature Factors (Å^2 × 100) with Esd's for $[Mn_2(\mu\text{-}O)_2(\mu\text{-}OAc)(H_2O)_2(bipy)_2](ClO_4)_3\cdot H_2O$

atom	*x*/*a*	*y*/*b*	*z*/*c*	U_{eq}[a]
Mn(1)	0.51251(2)	0.25089(2)	0.40419(2)	3.07(5)
Mn(2)	0.64576(2)	0.22128(2)	0.32570(2)	3.03(5)
Ow(1)	0.5385(1)	0.2547(1)	0.5329(1)	4.7(3)
Ow(2)	0.6297(1)	0.1863(1)	0.2041(1)	4.7(3)
O(1)	0.6545(1)	0.25107(9)	0.43413(9)	3.1(2)
O(2)	0.5065(1)	0.24679(9)	0.29178(9)	3.1(2)
O(3)	0.5039(1)	0.13203(9)	0.4075(1)	4.1(3)
O(4)	0.6224(1)	0.10748(9)	0.3456(1)	4.1(3)
C(1)	0.5567(2)	0.0841(1)	0.3794(2)	4.0(4)
C(2)	0.5410(2)	–0.0067(1)	0.3850(2)	5.8(5)
N(1)	0.4996(1)	0.3738(1)	0.4013(1)	3.6(3)
C(3)	0.3989(2)	0.4040(1)	0.3674(2)	4.0(4)
C(4)	0.3826(2)	0.4882(2)	0.3569(2)	5.3(5)
C(5)	0.4688(3)	0.5402(2)	0.3820(2)	6.1(5)
C(6)	0.5710(2)	0.5090(2)	0.4189(2)	5.5(5)
C(7)	0.5842(2)	0.4251(2)	0.4277(2)	4.6(4)
N(2)	0.3517(1)	0.2634(1)	0.3647(1)	3.9(3)
C(8)	0.3158(2)	0.3418(2)	0.3467(2)	3.9(4)
C(9)	0.2073(2)	0.3586(2)	0.3121(2)	5.5(5)
C(10)	0.1374(2)	0.2948(2)	0.2977(2)	6.6(6)
C(11)	0.1733(2)	0.2151(2)	0.3163(2)	6.3(5)
C(12)	0.2830(2)	0.2002(2)	0.3506(2)	5.0(4)
N(3)	0.6880(1)	0.3327(1)	0.2973(1)	4.0(3)
C(13)	0.7950(2)	0.3480(2)	0.3335(2)	5.1(4)
C(14)	0.8315(2)	0.4239(2)	0.3225(2)	6.1(5)
C(15)	0.7616(2)	0.4826(2)	0.2757(2)	6.2(5)
C(16)	0.6529(2)	0.4663(2)	0.2381(2)	6.0(5)
C(17)	0.6187(2)	0.3892(2)	0.2497(2)	5.4(5)
N(4)	0.6880(1)	0.3327(1)	0.2973(1)	4.0(3)
C(18)	0.8618(2)	0.2784(2)	0.3789(2)	5.0(4)
C(19)	0.9729(2)	0.2797(2)	0.4212(2)	5.1(4)
C(20)	1.0251(2)	0.2057(2)	0.4575(2)	5.6(5)
C(21)	0.9688(2)	0.1363(2)	0.4536(2)	6.6(6)
C(22)	0.8596(2)	0.1380(2)	0.4137(2)	5.4(5)
Cl(1)	0.33300(4)	0.26527(4)	0.62223(4)	4.9(1)
O(5)	0.2512(2)	0.2226(2)	0.6385(2)	9.5(5)
O(6)	0.3989(2)	0.2026(1)	0.6060(2)	10.2(5)
O(7)	0.2891(2)	0.3116(2)	0.5419(2)	9.0(5)
O(8)	0.3940(2)	0.3165(2)	0.6968(2)	9.9(6)
Cl(2)	0.31569(6)	0.47445(5)	0.10564(5)	6.4(1)
O(9)	0.3510(2)	0.3946(2)	0.1197(2)	11.5(7)
O(10)	0.3048(2)	0.5104(2)	0.0227(2)	9.1(5)
O(11)	0.2335(2)	0.4901(2)	0.1307(2)	11.3(6)
O(12)	0.4047(2)	0.5183(2)	0.1673(2)	12.4(8)
Cl(3)	0.38857(5)	0.06607(5)	0.10081(5)	5.8(1)
O(13)	0.3372(2)	0.0113(2)	0.0353(2)	12.8(7)
O(14)	0.4976(3)	0.0752(3)	0.1103(5)	11(1)
O(15)	0.3351(5)	0.1327(4)	0.0508(4)	11(1)
O(16)	0.3816(6)	0.0679(4)	0.1854(3)	10(1)
O(14)′	0.4404(4)	0.1367(4)	0.0861(3)	8(1)
O(15)′	0.3096(4)	0.0961(3)	0.1313(5)	10(1)
O(16)′	0.4577(4)	0.0196(4)	0.1716(3)	9(1)
Ow(3)	0.2354(2)	0.2579(2)	0.1389(1)	6.4(4)

[a] U_{eq} = $^1/_3$ of the trace of the orthogonalized $\mathbf{U}_{ij}$ tensor.

Table 3. Selected Interatomic Distances (Å) for $[Mn_2(\mu\text{-}O)_2(\mu\text{-}OAc)(H_2O)_2(bipy)_2](ClO_4)_3\cdot H_2O$

	Manganese Environment		
Mn(1)–O(1)	1.800(1)	Mn(2)–O(1)	1.787(2)
Mn(1)–O(2)	1.799(2)	Mn(2)–O(2)	1.804(1)
Mn(1)–O(3)	1.933(2)	Mn(2)–O(4)	1.921(2)
Mn(1)–Ow(1)	1.982(2)	Mn(2)–Ow(2)	1.985(2)
Mn(1)–N(1)	1.999(2)	Mn(2)–N(3)	2.004(2)
Mn(1)–N(2)	2.037(2)	Mn(2)–N(4)	2.049(2)
Mn(1)···Mn(2)	2.6401(5)		
	Acetate		
O(3)–C(1)	1.260(3)	O(4)–C(1)	1.277(3)
C(1)–C(2)	1.496(3)		
	Bipyridine		
N(1)–C(3)	1.354(3)	N(3)–C(13)	1.364(3)
C(3)–C(4)	1.382(3)	C(13)–C(14)	1.364(4)
C(4)–C(5)	1.371(4)	C(14)–C(15)	1.351(4)
C(5)–C(6)	1.379(4)	C(15)–C(16)	1.388(4)
C(6)–C(7)	1.372(3)	C(16)–C(17)	1.372(4)
C(7)–N(1)	1.347(3)	C(17)–N(3)	1.326(3)
C(3)–C(8)	1.453(3)	C(13)–C(18)	1.457(4)
N(2)–C(8)	1.352(3)	N(4)–C(18)	1.357(4)
C(8)–C(9)	1.386(3)	C(18)–C(19)	1.395(3)
C(9)–C(10)	1.363(4)	C(19)–C(20)	1.402(4)
C(10)–C(11)	1.373(5)	C(20)–C(21)	1.349(5)
C(11)–C(12)	1.396(3)	C(21)–C(22)	1.370(4)
C(12)–N(2)	1.344(3)	C(22)–N(4)	1.338(3)

methyl)-1,2-ethanediamine) (161.3(3)°) and confirms that the acetato bridge causes a bending of the $Mn^{IV}(\mu\text{-}O)_2Mn^{IV}$ unit resulting in a short Mn···Mn distance as previously observed for related binuclear compounds exhibiting a bis(μ-oxo), μ-acetato[8,13,26–29] or a bis(μ-oxo), μ-phosphato[15] central unit. The Mn···Mn distance (2.6401(5) Å), although at the lower range of those reported for other $Mn^{IV}(\mu\text{-}O)_2Mn^{IV}$ cores,[6e,13–15,30] agrees with the +4 manganese oxidation state and does not indicate any significant metal–metal bond.

One bpy and one water molecule complete the coordination around each manganese. The average Mn(1)–L distance is equal to the average Mn(2)–L distance (1.925 Å) with four Mn–N bonds ranging from 1.999(2) to 2.049(2) Å, four Mn–O bonds (oxide) ranging from 1.787(2) to 1.804(1) Å, two Mn–O distances (bridging acetate) of 1.921(2) and 1.933(2) Å and two Mn–O (water) distances of 1.982(2) and 1.985(2) Å, which clearly establish that the coordination geometries of the two manganese atoms are virtually identical. As observed for previously described μ-oxo-, μ-acetato-bridged manganese binuclear compounds,[31] the more strongly donating ligand (one arm of the bpy) coordinates trans to an oxo group, and as already observed for $[(phen)_2Mn^{IV}O_2Mn^{IV}(phen)_2](ClO_4)_4\cdot CH_3CN$,[6e] the equatorial Mn–N distances are significantly longer than the axial ones (Table 3), reflecting the trans influence of the bridging oxygen atoms on the equa torial nitrogen atoms. The presence of water in the coordination sphere of manganese(IV) is another interesting feature of this compound in which the above-described ligand set is sufficiently donating to stabilize high-valent metal centers to the extent that coordinating water remains fully protonated. Deviations of manganese atoms from their least-squares coordination planes[32] are less than 0.0462(3) Å.

The crystallization water molecule, the three perchlorate anions, and the two manganese coordinated water molecules participate in a three-dimensional hydrogen-bonding network (Figure 2) including six different hydrogen contacts.[32]

Optical Spectroscopy. The Mn(IV,IV) complex is sparingly soluble in water. Dilute aqueous solutions are deep brown and are fairly stable. The complex also dissolves readily in solvents such as DMF, CH_3CN, and picolines to afford brown solutions. However, these solutions decolorize rapidly, depositing brown solids, probably MnO_2 (solvate). The electronic spectrum of the aqueous solution (Figure 3) shows a broad shoulder at 20 400

---

(27) Pal, S.; Chan, M. K.; Armstrong, W. H. *J. Am. Chem. Soc.* **1992**, *114*, 6398–6406.

(28) Pal, S.; Gohdes, J. W.; Wilisch, W. C. A.; Armstrong, W. H. *Inorg. Chem.* **1992**, *31*, 713–716.

(29) Wieghardt, K.; Bossek, U.; Zsolnai, L.; Huttner, G.; Blondin, G.; Girerd, J. J.; Babonneau, F. *J. Chem. Soc., Chem. Commun.* **1987**, 651–653.

(30) (a) Libby, E.; Webb, R. J.; Streib, W. E.; Li, Q.; Folting, K.; Huffman, J. C.; Hendrickson, D. N.; Christou, G. *Inorg. Chem.* **1989**, *28*, 4037–4040. (b) Auger, N.; Girerd, J. J.; Corbella, M.; Gleizes, A.; Zimmermann, J. L. *J. Am. Chem. Soc.* **1990**, *112*, 448–450. (c) Goodson, P. A.; Glerup, J.; Hodgson, D. J.; Michelsen, K.; Pedersen, E. *Inorg. Chem.* **1990**, *29*, 503–508. (d) Oki, A. R.; Glerup, J.; Hodgson, D. J. *Inorg. Chem.* **1990**, *29*, 2435–2441. (e) Goodson, P. A.; Glerup, J.; Hodgson, D. J.; Michelsen, K.; Weihe, H. *Inorg. Chem.* **1991**, *30*, 4909–4914. (f) Gohdes, J. W.; Armstrong, W. H. *Inorg. Chem.* **1992**, *31*, 368–373. (g) Larson, E.; Lah, M. S.; Li, X.; Bonadies, J. A.; Pecoraro, V. L. *Inorg. Chem.* **1992**, *31*, 373–378.

(31) Thorp, H. H.; Brudvig, G. W. *New J. Chem.* **1991**, *15*, 479–490.

(32) Supplementary material.

Table 4. Selected Interatomic Angles (deg) for $[Mn_2(\mu\text{-}O)_2(\mu\text{-}OAc)(H_2O)_2(bipy)_2](ClO_4)_3{\cdot}H_2O$

Manganese Environment			
O(1)–Mn(1)–O(2)	83.76(6)	O(1)–Mn(2)–O(2)	83.99(6)
O(1)–Mn(1)–O(3)	93.70(7)	O(1)–Mn(2)–O(4)	92.55(7)
O(1)–Mn(1)–Ow(1)	89.22(7)	O(1)–Mn(2)–Ow(2)	177.50(7)
O(1)–Mn(1)–N(1)	94.58(7)	O(1)–Mn(2)–N(3)	94.02(8)
O(1)–Mn(1)–N(2)	173.66(8)	O(1)–Mn(2)–N(4)	89.52(7)
O(2)–Mn(1)–O(3)	90.73(7)	O(2)–Mn(2)–O(4)	92.77(7)
O(2)–Mn(1)–Ow(1)	172.97(6)	O(2)–Mn(2)–Ow(2)	93.94(7)
O(2)–Mn(1)–N(1)	92.54(8)	O(2)–Mn(2)–N(3)	94.92(7)
O(2)–Mn(1)–N(2)	93.90(7)	O(2)–Mn(2)–N(4)	171.60(8)
O(3)–Mn(1)–Ow(1)	89.35(8)	O(4)–Mn(2)–Ow(2)	86.13(7)
O(3)–Mn(1)–N(1)	171.38(8)	O(4)–Mn(2)–N(3)	170.37(9)
O(3)–Mn(1)–N(2)	92.22(7)	O(4)–Mn(2)–N(4)	92.85(8)
Ow(1)–Mn(1)–N(1)	88.38(8)	Ow(2)–Mn(2)–N(3)	87.55(8)
Ow(1)–Mn(1)–N(2)	93.12(7)	Ow(2)–Mn(2)–N(4)	92.67(8)
N(1)–Mn(1)–N(2)	79.61(8)	N(3)–Mn(2)–N(4)	80.18(8)
Mn(1)–O(1)–Mn(2)	94.79(5)	Mn(1)–O(2)–Mn(2)	94.24(5)
Acetate			
Mn(1)–O(3)–C(1)	123.7(2)	Mn(2)–O(4)–C(1)	123.2(2)
O(3)–C(1)–O(4)	124.7(2)	O(3)–C(1)–C(2)	118.0(3)
O(4)–C(1)–C(20)	117.3(2)		
Bipyridine			
Mn(1)–N(1)–C(7)	123.5(2)	Mn(2)–N(3)–C(17)	123.7(2)
Mn(1)–N(1)–C(3)	115.8(1)	Mn(2)–N(3)–C(13)	114.8(1)
C(7)–N(1)–C(3)	120.7(2)	C(17)–N(3)–C(13)	121.4(2)
N(1)–C(3)–C(4)	119.7(2)	N(3)–C(13)–C(14)	119.4(2)
C(3)–C(4)–C(5)	119.5(2)	C(13)–C(14)–C(15)	119.8(3)
C(4)–C(5)–C(6)	120.4(2)	C(14)–C(15)–C(16)	120.5(3)
C(5)–C(6)–C(7)	118.5(3)	C(15)–C(16)–C(17)	118.3(2)
C(6)–C(7)–N(1)	121.2(2)	C(16)–C(17)–N(3)	120.5(3)
N(1)–C(3)–C(8)	114.6(2)	N(3)–C(13)–C(18)	115.3(2)
C(4)–C(3)–C(8)	125.7(2)	C(14)–C(13)–C(18)	125.3(2)
N(2)–C(8)–C(3)	114.8(2)	N(4)–C(18)–C(13)	114.9(2)
C(3)–C(8)–C(9)	124.5(2)	C(13)–C(18)–C(19)	125.4(3)
Mn(1)–N(2)–C(12)	124.6(2)	Mn(2)–N(4)–C(22)	124.4(2)
Mn(1)–N(2)–C(8)	114.5(1)	Mn(2)–N(4)–C(18)	113.7(2)
C(12)–N(2)–C(8)	120.7(2)	C(22)–N(4)–C(18)	121.4(2)
N(2)–C(8)–C(9)	120.6(2)	N(4)–C(18)–C(19)	119.6(2)
C(8)–C(9)–C(10)	118.9(3)	C(18)–C(19)–C(20)	117.9(3)
C(9)–C(10)–C(11)	120.8(2)	C(19)–C(20)–C(21)	120.6(2)
C(10)–C(11)–C(12)	118.9(3)	C(20)–C(21)–C(22)	119.8(3)
C(11)–C(12)–N(2)	120.1(3)	C(21)–C(22)–N(4)	120.6(3)

cm^{-1} which may be compared with the shoulder observed in the same region for other $Mn^{IV}(\mu\text{-}O)_2Mn^{IV}$ complexes containing ligands like phenanthroline,[6e] *N,N'*-bis(2-pyridylmethyl)-1,2-ethanediamine,[30c] *N,N',N''*-trimethyl-1,4,7-triazacyclononane[33] and 1,2-bis(5-chlorosalicylideneamino)ethane.[34]

When the complex is dissolved in bipy/bipyHNO$_3$ buffer (pH 4.5), the electronic spectrum gradually changes to that of the mixed-valent $[Mn_2(O)_2(bipy)_4]^{3+}$ with maxima at 672 (ϵ = 450 M^{-1} cm^{-1}) and 552 nm (ϵ = 360 M^{-1} cm^{-1}). Absorptions in this region were observed for other $Mn^{III}Mn^{IV}$ binuclear compounds.[30c] It has been suggested that oxo to Mn(IV) $d\pi^*$ charge-transfer transitions account for these distinctive bands.[30d] However, in the case of bipy[6c] and cyclam[35] dimers, similar bands have been assigned to d–d transitions. On the basis of the extinction coefficient of the intervalence absorption band, nearly 80% of the Mn is present as the $Mn^{III}Mn^{IV}$ complex after 72 h (Figure 3).

Magnetic Properties. The temperature dependence of the magnetic susceptibility and effective magnetic moment per manganese of the Mn^{IV}_2 complex are shown in Figure 4. μ_{eff}/Mn decreases from 2.91 μ_B at 325 K to 0.77 μ_B at 15 K, indicating an antiferromagnetic coupling of the $S = {}^3/_2$ spin systems of the two manganese(IV) ions of this binuclear species. However, the room-temperature value of 2.83 clearly indicates that the antiferromagnetic interaction operating in this compound is lower than that measured for most other binuclear Mn^{IV}_2 complexes.[6e,27,30,36] The data were fitted by employing the expression derived from the isotropic spin-exchange Hamiltonian $\mathcal{H} = -2JS_1S_2$ ($S_1 = S_2 = {}^3/_2$) and the Van Vleck equation.[37] Least-

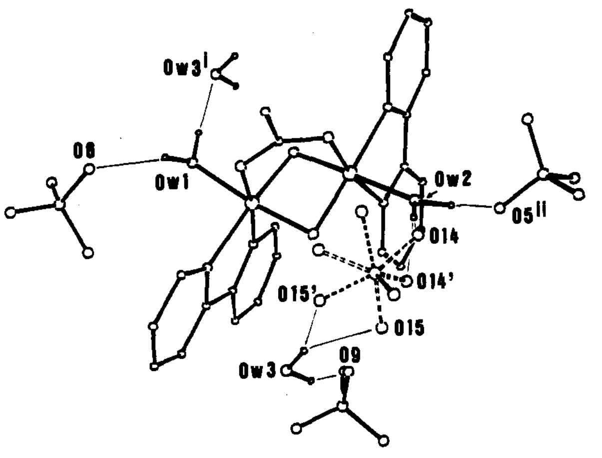

Figure 2. Perspective view of the $[Mn_2(\mu\text{-}O)_2(\mu\text{-}OAc)(H_2O)_2(bipy)_2](ClO_4)_3{\cdot}H_2O$ molecule showing the three-dimensional hydrogen bond network.

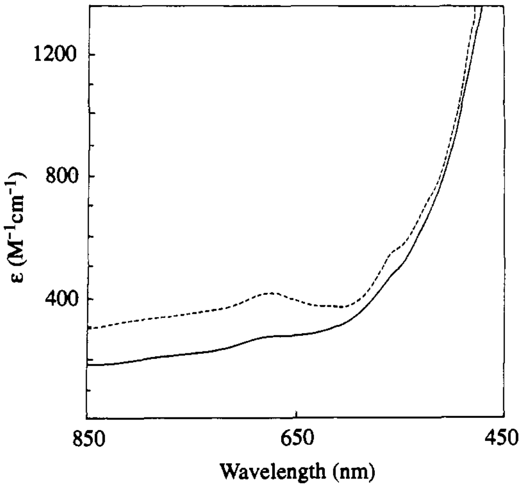

Figure 3. Electronic spectrum of $[Mn_2(\mu\text{-}O)_2(\mu\text{-}OAc)(H_2O)_2(bipy)_2](ClO_4)_3{\cdot}H_2O$ in bipyridine buffer at pH 4.5: (—) initial compound; (- - -) compound after 72 h.

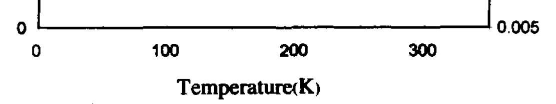

Figure 4. Variable-temperature magnetic susceptibility data for $[Mn_2(\mu\text{-}O)_2(\mu\text{-}OAc)(H_2O)_2(bipy)_2](ClO_4)_3{\cdot}H_2O$. The solid lines result from a least-squares fit of the data to the theoretical magnetic susceptibility calculated as mentioned in the text.

---

(33) Wieghardt, K.; Bossek, U.; Naber, B.; Weiss, J.; Bonvoisin, J.; Corbella, M.; Vitols, S. E.; Girerd, J. J. *J. Am. Chem. Soc.* **1988**, *110*, 7398–7411.

(34) Dailey, G. C.; Horwitz, C. P.; Lisek, C. A. *Inorg. Chem.* **1992**, *31*, 5325–5330.

(35) Brewer, K. J.; Calvin, M.; Lumpkin, R. S.; Otvos, J. W.; Spreer, L. O. *Inorg. Chem.* **1989**, *28*, 4446–4451.

(36) Suzuki, M.; Tokura, S.; Suhara, M.; Uehara, A. *Chem. Lett.* **1988**, 477–480.

(37) O'Connor, C. J. *Prog. Inorg. Chem.* **1982**, *29*, 203–283.

Table 5. Selected Structural and Magnetic Parameters for Compounds Including a $Mn^{IV}(\mu\text{-}O)_2Mn^{IV}$ Core

compound								
no.	formula	Mn–μ–O, Å	Mn···Mn, Å	Mn–O–Mn, deg	α, deg	J, cm^{-1}	g	ref
1	$[Mn_2(\mu\text{-}O)_2(phen)_2]^{4+}$	1.801(4)	2.748(2)	99.5(2)	180	−144	1.96	6e
2	$[Mn_2(\mu\text{-}O)_2(pic)_2]$	1.819(3)	2.747(2)	98.1(2)	180	−86.5	1.83	30a
3	$[Mn_2(\mu\text{-}O)_2(bispicen)_2]^{4+}$	1.811(3)	2.676(2)	95.2(2)	180	−125.5	1.95	30c
4	$[Mn_2(\mu\text{-}O)_2(dmepa)_2]^{4+}$	1.78(3)	2.75(2)	101.5(2)	180	−131		30d
5	$[Mn_2(\mu\text{-}O)_2(bispictn)_2]^{4+}$	1.803(8)	2.719(3)	97.8(4)	180	−105.5	1.83	30e
6	$[Mn_2(\mu\text{-}O)_2(salpn)_2]$	1.819(3)	2.728(1)	97.2(1)	180	−82	1.79	30f
7	$[Mn_2(\mu\text{-}O)_2(\mu\text{-}HPO_4)(bipy)_2(H_2PO_4)_2]$	1.810(5)	2.702(2)	96.5(4)	164.5	−39.5	1.81	15, 38
8	$[Mn_2(\mu\text{-}O)_2(\mu\text{-}OAc)(tpen)]^{3+}$	1.798(3)	2.591(1)	92.2(2)	161.3			26
9	$[Mn_2(\mu\text{-}O)_2(\mu\text{-}OAc)(bpea)]^{3+}$	1.799(4)	2.580(1)	91.6(2)	164.8	−124	2.29	27
10	$[Mn_2(\mu\text{-}O)_2(\mu\text{-}OAc)(bipy)_2(H_2O)_2]^{3+}$	1.797(1)	2.6401(5)	94.51(5)	161.7	−43.7	1.976	this work

squares refinement afforded an excellent fit with $J = -43.7$ cm^{-1}, Par = 3.5%, TIP = 0, and $g = 1.976$, where Par is the mole percent of a paramagnetic impurity assumed to be a Mn(II) monomer and TIP is the temperature-independent paramagnetism. Equally good fits were obtained for g values ranging from 1.93 to 1.99 with minor variations of J (±0.5 cm^{-1}). This result is very similar to that reported very recently for $[Mn^{IV}_2(\mu\text{-}O)_2(\mu\text{-}HPO_4)(bipy)_2(H_2PO_4)_2]$ ($J = -39.5$ cm^{-1}),[38] and the exchange integral for both compounds is much weaker than that obtained for all other binuclear Mn(IV) compounds including a $(\mu\text{-}O)_2$ bridge.

As recently commented,[27] the exchange integral J for the structurally characterized species containing the $Mn^{IV}(\mu\text{-}O)_2$-Mn^{IV} core does not correlate with Mn–μ-O and/or Mn···Mn distances and/or Mn–μ-O–Mn angles and these additional examples seem to confirm the lack of correlation between J and the structural parameters supposed to better reflect the direct d_{xy}–d_{xy} orbital overlap (x and y axes coincident with the Mn–μ-O bonds). In their recent paper, Sarneski *et al.*[38] have referred to the interpretation proposed by Hendrickson *et al.*[30a] to explain the weak exchange integral obtained for $[Mn^{IV}_2(\mu\text{-}O)_2(\mu\text{-}HPO_4)(bipy)_2(H_2PO_4)_2]$. However, it should be noted that although both Sarneski's and Hendrickson's binuclear Mn(IV) compounds are characterized by similar N_2O_4 to manganese donor sets, the strength of the antiferromagnetic interaction in the $[Mn^{IV}_2(\mu\text{-}O)_2(picolinate)_4]$ complex ($J = -86.5$ cm^{-1})[30a] is more than twice as large as that measured for $[Mn^{IV}_2(\mu\text{-}O)_2(\mu\text{-}HPO_4)(bipy)_2(H_2PO_4)_2]$ ($J = -39.5$ cm^{-1}).[38] As the number of π-bonding oxygen ligands is the same in both complexes, the energy mismatch between the d_π orbitals and the bridging oxide p_π orbitals should not be considerably different, eventhough the oxygen donor atom of the picolinate and of the phosphate have a different π-bonding character.

It seems thus clear that if the ratio of O-based versus N-based ligation probably acts indirectly upon the strength of the antiferromagnetic interaction in the $Mn^{IV}(\mu\text{-}O)_2Mn^{IV}$ core, this factor cannot account by itself for the variations observed among the 10 binuclear compounds presently known to include this core. In these respects, a detailed analysis of the magnetic interactions and structural parameters for the 10 compounds gathered in Table 5 is of interest although the exchange integral J is not yet available for one of them. The binuclear Mn(IV,IV) compounds in Table 5 clearly include two distinct sets with respect to the values of the dihedral angle α between μ-O(1)Mn(1)–μ-O(2) and μ-O(1)-Mn(2)–μ-O(2) reflecting the departure of the $Mn^{IV}(\mu\text{-}O)_2Mn^{IV}$ ring from planarity: (i) those with α values equal or very close to 180° (**1**–**6**) and (ii) those with α values departing noticeably from 180° (**7**–**10**). As the direct d_{xy}–d_{xy} orbital overlap should be optimal when the xy plane is the same for both Mn atoms, the weakening of the antiferromagnetic interaction could be correlated to the departure of α from 180° as recently evidenced in a series of μ-alkoxo-bridged binuclear manganese compounds.[39]

The α values being very close to each other inside each set of compounds, the direct d_{xy}–d_{xy} orbital overlap should be the same inside each set and a decrease in J values should parallel an increase of O-based versus N-based ligation inside each set. This is indeed the case as **1**, **3**, **4**, and **5** (α = 180°, N_4O_2 donor sets) experience antiferromagnetic interactions ranging from −144 to −105.5 cm^{-1} while **2** and **6** (α = 180°, N_2O_4 donor sets) experience antiferromagnetic interactions of −86.5 and −82 cm^{-1}, respectively. Similarly, **9** (α = 164.8°, N_3O_3 donor set) is characterized by a −124 cm^{-1} exchange integral while **7** and **10** (α = 164.5 and 161.7°, N_2O_4 donor sets) are characterized by −39.5 and −43.7 cm^{-1} exchange integrals respectively.

However, this first type of comparison shows that (i) the range of J values for **1**, **3**, **4**, and **5** is large (38.5 cm^{-1}) and (ii) the average decrease in J between compounds with N_4O_2 and N_2O_4 donor sets (44.5 cm^{-1}) is smaller than the average decrease in J between compounds with N_3O_3 and N_2O_4 donor sets (82.5 cm^{-1}). These apparent peculiarities may originate in the intervention of secondary structural and/or electronic factor(s) not assessed in this rough analysis. Moreover, the J values for compounds **1**–**10** would be strictly comparable only to the condition that g variations are small enough to prevent compensating effects, and this condition is not completely fulfilled as shown by the following examples. Compounds **2** and **6**, which exhibit the less negative J exchange parameters within the first set of compounds, are also characterized by the smaller g values. On the same lines, when the magnetic susceptibility data of **5** are fitted by using the usual $-2JS_1S_2$ formalism, the parameters obtained are $J = -105.5$ cm^{-1} and $g = 1.83$, while fitting the same data to the equation for an exchange coupled dimer including a biquadratic term affords the parameters $J = -148$ cm^{-1}, $j = -11$ cm^{-1}, and $g = 1.95$.[30e] Similarly, the surprisingly strong antiferromagnetic coupling in **9** is associated with an unusually high g value. Another factor that hampers J comparisons arises from the presence of non-negligible amounts of low-valent paramagnetic impurities (Par) in all these high-valent bis(μ-oxo)-bridged manganese compounds.

Despite these apparent peculiarities and taking into account the uncertainties resulting from the diversity of the fitting protocols used, it is clear that a decrease in J values parallels an increase of O-based versus N-based ligation inside each set, thus validating Hendrickson's interpretation.

Comparison between compounds characterized by similar donor sets and different α values should evidence a possible correlation between the departure of α from 180° and a weakening of the antiferromagnetic interaction. In this respect, the J values for **2** and **6** (α = 180°, N_2O_4 donor sets) which are close to each other and average to −84 cm^{-1} while the J values for **7** and **10** ($\alpha \sim$ 163°, N_2O_4 donor sets), also close to each other, average to −41.5 cm^{-1} clearly indicate that the weakening of the antiferromagnetic interaction is correlated to the departure of α from 180°.

---

[38] Sarneski, J. E.; Brzezinski, L. J.; Anderson, B.; Didiuk, M.; Manchanda, R.; Crabtree, R. H.; Brudvig, G. W.; Schuttle, G. K. *Inorg. Chem.* **1993**, *32*, 3265–3269.

[39] Mikuriya, M.; Yamato, Y.; Tokii, T. *Bull. Chem. Soc. Jpn.* **1992**, *65*, 2624–2637.

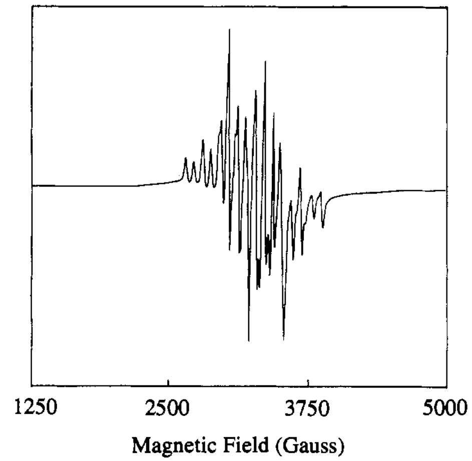

Figure 5. X-Band DMF glass EPR spectrum of $[Mn_2(\mu\text{-}O)_2(\mu\text{-}OAc)(H_2O)_2(bipy)_2](ClO_4)_3{\cdot}H_2O$ (T = 163 K; microwave frequency 9.207 GHz).

Examination of Table 5 shows that further substantiation of this correlation could be gained from the preparation and study of $Mn^{IV}(\mu\text{-}O)_2Mn^{IV}$ compounds with $\alpha = 180°$ and N_3O_3 donor sets, to allow comparison with **9**. The study of the magnetic properties of **8** would also be valuable in this respect as the exchange integral evaluated for **9** is unexpectedly large.

EPR Spectroscopy. The 300 K, X-band, powder EPR spectrum of $[Mn_2(\mu\text{-}O)_2(\mu\text{-}OAc)(H_2O)_2(bipy)_2](ClO_4)_3{\cdot}H_2O$ (finely ground crystals) exhibits a main $g \sim 2$ centered resonance with a ill-defined six-line hyperfine structure and several weak resonances ranging from 0 to 6000 G. On lowering the temperature, the main $g \sim 2$ resonance broadens and the ^{55}Mn hyperfine splitting is lost while the intensity of the surrounding weak fine structure resonances increases. The presence of a six-line hyperfine structure indicates that the main resonance arises at least partly from a mononuclear Mn(IV) or Mn(II) impurity. The presence of a paramagnetic impurity in the ground crystals is confirmed by the magnetic susceptibility measurements, the analysis of which indicates it to be 3.5%, if the impurity is assumed to be Mn(II).

The glass EPR spectrum of a freshly prepared DMF solution (Figure 5) clearly shows the formation of the $Mn^{III}Mn^{IV}$ and Mn(II) species.[40] The solution reactions are therefore quite complex. It appears that solvent molecules are able to displace the coordinated H_2O and the bridging acetate and the resulting substituted complex decomposes gradually to MnO_2, $Mn^{III}Mn^{IV}$ and Mn(II) species, oxidizing water or the solvent. In the presence of added bipyridine, $[Mn_2(O)_2(bpy)_4]^{3+}$ is formed and further decomposition is prevented.

Concluding Remarks

$[Mn_2(\mu\text{-}O)_2(\mu\text{-}OAc)(H_2O)_2(bipy)_2](ClO_4)_3{\cdot}H_2O$ is the second compound in which water is found in the coordination sphere of manganese(IV). In the case of $[Mn^{IV}_3(O)_4(2,2'\text{-}bipy)_4(H_2O)_2](ClO_4)_4$,[14] the stabilization of the water molecules was attributed to the presence of a strongly donating ligand set (one bipy group and three bridging oxo groups) in the environment of the Mn(IV) centers to which the aquo moieties are ligated. The situation is not basically different in the $Mn^{IV}(\mu\text{-}O)_2(\mu\text{-}OAc)Mn^{IV}$ compound under study where the ligand set of the Mn(IV) centers includes one bipy group, two bridging oxo groups, and a μ-carboxylato oxygen atom. This new example indicates that the stabilization of water molecules in the environment of high-valent manganese is probably not exceptional. Consequently, these results are consistent with recent reports suggesting that the S_1 and S_2 states would include respectively a 2Mn(III)/2Mn(IV) and a Mn(III)/3Mn(IV) center.[41]

The $Mn^{IV}(\mu\text{-}O)_2(\mu\text{-}OAc)Mn^{IV}$ compound under study and $[Mn^{IV}_2(\mu\text{-}O)_2(\mu\text{-}HPO_4)(bipy)_2(H_2PO_4)_2]$[38] are characterized by the weakest antiferromagnetic interactions determined for bis(μ-oxo)-bridged Mn(IV) dimers which seems related to the fact that the departure of the $Mn^{IV}(\mu\text{-}O)_2Mn^{IV}$ ring from planarity is large (~17°) in both compounds. If this strong correlation is confirmed by further examples, it can give an insight into the role of conformational changes with respect to large modifications of magnetic interactions in metalloproteins.

Note Added in Proof. A communication describing succinctly the same compound obtained through a different synthetic route has been published very recently.[42]

Acknowledgment. K.R.R. thanks the University Grants Commission, New Delhi, for a senior fellowship. S.P. would like to acknowledge USEFI/India for a travel fellowship and Dr. Wayne Frasch, Center for Study of Eearly Events in Photosynthesis at Arizona State University, for Hospitality.

Supplementary Material Available: Tables giving complete crystal data and experimental details, components of the anisotropic temperature factors, hydrogen atomic positional and thermal parameters, bond lengths and angles, least-squares planes and deviations of atoms therefrom (9 pages). Ordering information is given on any current masthead page.

---

[40] Mn^{III}_2 or Mn^{IV}_2 species cannot account for a 16-line spectrum with irregular intensity pattern in the middle. However, this spectrum can be accounted for by overlap of the $Mn^{III}Mn^{IV}$ multiline signal with the usual six-line Mn(II) absorption: Swarnabala, G.; Rajasekharan, M. V. *Inorg. Chim. Acta* **1990**, *168*, 167.

[41] (a) Yachandra, V. K.; DeRose, V. J.; Latimer, M. J.; Mukerji, I.; Sauer, K.; Klein, M. P. *Science* **1993**, *260*, 675–679. (b) Philouze, C.; Blondin, G.; Ménage, S.; Auger, N.; Girerd, J. J.; Vigner, D.; Lance, M.; Nierlich, M. *Angew. Chem., Int. Ed. Engl.* **1992**, *31*, 1629–1631 and references therein.

[42] Dave, B. C.; Czernuszewicz, R. S.; Bond, M. C.; Carrano, C. J. *Inorg. Chem.* **1993**, *32*, 3593.